KEK Preprint 98-201
KUNS-1547
December 1998
H

Emission Angle Dependence of the Nuclear Temperature and Free Nucleon Density in Light Projectile-Induced Reactions

J. MURATA. M. HASENO, K. KIMURA, F. KOSUGE, R. KUBOHARA, S. MIHARA, S. MORINOBU, T. MURAKAMI, R. MURAMATSU, Y. NAGASAKA, K. NAKAI, H. OCHIISHI, Y. OHKUMA, Y. OKUNO, T. SHIBATA, Y. SHIBATA, Y. SUGAYA, K. H. TANAKA, Y. TANAKA, Y. J. TANAKA, K. USHIE, Y. YAMANOI and K. YASUDA

Submitted to Physical Review C (Rapid Communication).

High Energy Accelerator Research Organization (KEK), 1998

KEK Reports are available from:

Information Resources Division
High Energy Accelerator Research Organization (KEK)
1-1 Oho, Tsukuba-shi
Ibaraki-ken, 305-0801
JAPAN

Phone: 0298-64-5137
Fax: 0298-64-4604
Cable: KEK OHO
E-mail: Library@kekvax.kek.jp
Internet: http://www.kek.jp

Emission Angle Dependence of the Nuclear Temperature and Free Nucleon Density in Light Projectile-Induced Reactions

J. Murata,[1] M. Haseno,[2] K. Kimura,[2] F. Kosuge,[3] R. Kubohara,[3] S. Mihara,[1] *
S. Morinobu,[4] T. Murakami,[1] R. Muramatsu,[1] Y. Nagasaka,[2] K. Nakai,[3] H. Ochiishi,[4]
Y. Ohkuma,[5] Y. Okuno,[2] T. Shibata,[6] Y. Shibata,[3] Y. Sugaya,[7] † K. H. Tanaka,[6]
Y. Tanaka,[2] Y. J. Tanaka,[1] K. Ushie,[2] Y. Yamanoi,[6] and K. Yasuda[1]
(MULTI Collaboration)

[1] *Department of Physics, Kyoto University, Kyoto 606-8502, Japan*

[2] *Nagasaki Institute of Applied Science, Nagasaki 851-0193, Japan*

[3] *Faculty of Science and Technology, Science University of Tokyo, Chiba 278-8510, Japan*

[4] *Department of Physics, Kyushu University, Fukuoka 812-8581, Japan*

[5] *Institute of Physics, University of Tsukuba, Tsukuba 305-8571, Japan*

[6] *Institute of Particle and Nuclei Studies, KEK, Tsukuba 305-0801, Japan*

[7] *Tokyo University of Agriculture and Technology, Tokyo 184-8588, Japan*

Abstract

The fragment emission-angle dependence of the nuclear temperature and free nucleon density has been measured for the first time in 8-GeV and 12-GeV proton-induced target multi-fragmentation reactions on various targets. The isotope-yield ratios have been used to extract the temperature and free-nucleon density. "U-Shape" angular distributions have been observed for both of them. This fact suggests that the temperature and density distributions in the emission source of intermediate mass fragments (IMFs) should not be uniform. The existence of nonuniformity could be the origin of the reported sideward-yield enhancement of the IMF production.

25.70.Pq, 25.40.Ve, 21.65.+f, 24.0.Pa

*Present address: International Center for Elementary Particle Physics(ICEPP), University of Tokyo, Tokyo 113-0033, Japan

†Present address: Research Center for Nuclear Physics (RCNP), Osaka University, Suita 567-0047, Japan

Over the last few decades a considerable number of studies have been made on extracting nuclear temperatures from experimental data of intermediate and relativistic energy heavy-ion collisions.[1] The main purpose of those temperature measurements is to search for a signal of a nuclear liquid-gas phase transition. Temperature measurements using the isotope-yield ratios have recently been brought to light by determining the "caloric curve" for nuclear matter.[2] One advantage of this method is its experimental simplicity. The isotope temperature, as a probe for the chemical freeze-out temperature, can be obtained only by forming isotope-yield ratios.[3] We can also determine the free-proton and free-neutron densities at the same time. Recently, we have observed sideward-peaked angular distributions for IMF production in interactions between the 12-GeV proton and heavy nuclei,[4] which implies that the entire fragment emission source might not be thermally equilibrated. It would be therefore extremely important to investigate the emission angle dependence of the temperature and nucleon densities, which have been considered to be isotropic in past studies, in order to understand the excitation mechanism in the multi-fragmentation reaction. In this paper we report on results from the first measurements of angular distributions for the temperature and free-nucleon densities in GeV-energy light-projectile induced multi-fragmentation reactions. We observed anisotropic angular distributions for them, suggesting that the emission source of IMFs is not fully equilibrated at the chemical freeze out, and that the fragment density in the source would also be nonuniform. This nonuniform fragment density could be the origin of the sideward peaked angular distributions for IMF production.

The experiments were performed at the High Energy Accelerator Research Organization Proton Synchrotron (KEK-PS) with 8-GeV and 12-GeV primary proton beams. Three targets (Au, Sm, and Ag) and four targets (Au, Tm, Sm, and Ag) of about 600 μg/cm^2 thickness were used in 8-GeV and 12-GeV $p+A$ reactions, respectively. IMFs of $3 \leq Z \leq 30$ emitted from the target were detected by Bragg Curve Counters (BCCs), which determined their charge numbers (Bragg peaks), kinetic energies, and ranges.[5] There were 37 BCCs surrounding the foil targets. Their total acceptance was about 20% of 4π. Each BCC had almost the same solid angle. 12 BCCs were located within the horizontal plane containing

the target. They covered an angular range of 30° to 150° at a step of 20° in the laboratory system for measuring the angular distributions and in-plane correlations. In order to collect information about the out-of-plane correlations and any IMF-multiplicity, a large conical-shape BCC array, consisting of 25 independent BCC channels, was located above the targets. Using the Bragg-peak information, IMFs could be individually identified with a charge separation of about 9σ. The excellent Bragg-peak resolution even split light fragments according to their mass difference.

In our experiment, ^{6,7,8,9}Li and ^{7,9,10}Be fragments were clearly separated in a Range vs. Energy plot, as shown in Fig. 1(a). The energy spectra of lithium and beryllium isotopes were obtained for inclusive, IMF-multiplicity=2 and =3 events (hereafter, we use abbreviations Inc., M2, and M3 for those events). Here, "IMF-multiplicity" denotes a raw hit-number of IMFs in the BCC array. In order to obtain continuous functions for the IMF differential cross sections, a moving-source model has been adopted to fit the energy spectra. Considering the existence of a sideward yield enhancement,[4] a sideward-deformation factor was introduced phenomenologically into the usual single moving source model, as follows:

$$\frac{d^2\sigma}{dEd\Omega} = N(\theta^*)\sqrt{E}exp(\frac{E^*}{T})\frac{1}{exp[\frac{2\pi(E_c-E^*)}{\delta E_c}]+1},$$

$$N(\theta^*) = N_0 + N_f exp[-\frac{(\theta^*-\theta_f^*)^2}{2\sigma_f^{*2}}]. \quad (1)$$

Here, the variables with an asterisk represent those in the rest frame of the moving source. The moving source velocity β was also treated as a fitting parameter. E is the laboratory kinetic energy, θ^* is the emission angle of fragments, T is the temperature parameter, and E_c and δE_c are the coulomb-barrier parameters; θ_f^* and σ_f^* are the peak angle and width of the additional Gaussian deformation factor representing the sideward peaked enhancement; N_0 and N_f are the normalization constants corresponding to the isotropic component and the deformed sideward peaking component.

The obtained continuous differential cross sections for the lithium and beryllium isotopes are shown in Fig. 1(b) for the 8 GeV p+Au reaction as an example. They are almost independent of the IMF-multiplicity, with the exception of those for ^{6}Li and ^{7}Li. From this figure

it is obvious that there are significant shape differences among the angular distributions of isotopes. Stable isotopes show the "usual" sideward peaked enhancements, while unstable isotopes show rather "unusual" forward-peaked angular distributions. A sideward region of the emission source might, therefore, have a relatively low freeze-out temperature, because unstable fragment production should require a higher temperature environment than that for stable fragments. In other words, if the temperature distribution of the hot source is uniform, the angular distributions of the isotope yields must have the same shapes, as long as all fragments are produced in the same moving source. Although fitted results of β for the lithium and beryllium isotopes are distributed from 0.002 to 0.006, the influence on the shape of the angular distribution should be negligible because of their very small values. Similar differential cross sections were also observed for the other targets and 12-GeV proton-induced reactions.

Assuming that the fragment density $\rho(A,Z)$ for the emitted fragment with mass and charge number A and Z at the freeze-out is proportional to the experimental yield $Y(A,Z)$, a single isotope yield ratio between two fragments, $R = Y(A_1,Z_1)/Y(A_2,Z_2)$, can be expressed as follows:[3]

$$R = (\frac{\lambda^3}{2})^{\eta+\xi}\rho_{pF}^{\eta}\rho_{nF}^{\xi}\alpha exp\frac{\Delta B}{T}. \tag{2}$$

Here, ρ_{pF} and ρ_{nF} are the free-proton and -neutron densities in a mixed ideal gas of free nucleon and fragments with an equilibrium temperature of T, respectively. The indices η and ξ are defined as $\eta = Z_1 - Z_2$ and $\xi = (A_1 - Z_1) - (A_2 - Z_2)$; λ, α, and ΔB are the thermal nucleon wavelength, $\lambda = h/\sqrt{2\pi mT}$, the statistical weight factor, $\alpha = (A_1/A_2)^{3/2}\omega(A_1,Z_1)/\omega(A_2,Z_2)$, and the binding energy difference, $\Delta B = B(A_1,Z_1) - B(A_2,Z_2)$, respectively. Here, m and $\omega(A,Z)$ denote the mass of a nucleon and the internal partition function of the fragment (A,Z), respectively.

Three unknown quantities (T, ρ_{pF} and ρ_{nF}) can be extracted from three independent experimental single ratios. Since the fragment density can be expressed using T, ρ_{pF} and ρ_{nF} from four experimental isotope yields, we can also deduce T, ρ_{pF}, ρ_{nF} and the ratio

between $\rho(A,Z)$ and $Y(A,Z)$. The calculation is much more simple, however, using three independent single ratios.

Using 21 single ratios among the seven isotopes, there are 1284 possible combinations of three single ratios to extract the temperature and nucleon densities at the same time. From them we could obtain 230 independent temperatures. T can be written as

$$T = \sum_{i=1,3} a_i\Delta B_i/ln\prod_{i=1,3}(R_i/\alpha_i)^{a_i}$$
$$= \frac{B_{multi}}{ln(R_{multi}/\alpha)}, \tag{3}$$

where $a_i = \xi_j\eta_k - \xi_k\eta_j$ for (i,j,k) =cyclic order of $(1,2,3)$, $B_{multi} = \sum_{i=1,3} a_i\Delta B_i$, $R_{multi} = \prod_{i=1,3} R_i^{a_i}$, and $\alpha = \prod_{i=1,3}\alpha_i^{a_i}$. The subscript i represents a variable with i related to the i-th single ratio. The free nucleon densities (ρ_{pF} and ρ_{nF}) can be expressed as

$$\rho_{pF} = \frac{2}{\lambda^3}[(\frac{R_i}{\alpha_i})^{\xi_j}(\frac{R_j}{\alpha_j})^{-\xi_i}exp(\frac{\Delta B_j\xi_i - \Delta B_i\xi_j}{T})]^{\frac{1}{\eta_i\xi_j - \eta_j\xi_i}}, \tag{4}$$

$$\rho_{nF} = \frac{2}{\lambda^3}[(\frac{R_i}{\alpha_i})^{\eta_j}(\frac{R_j}{\alpha_j})^{-\eta_i}exp(\frac{\Delta B_j\eta_i - \Delta B_i\eta_j}{T})]^{\frac{1}{\xi_i\eta_j - \xi_j\eta_i}}. \tag{5}$$

Using Eq. (3), 230 independent temperatures at 34° in the laboratory system have been calculated without any yield correction. In the calculation we took only the ground-state contribution into $\omega(A,Z)$. As can be seen in Fig. 2, the obtained temperatures are distributed over a wide range between $-10MeV < T < 30MeV$. If we select a large value of the quantity $\delta B = |\sum_i a_i\Delta B_i|/\sqrt{\sum_i a_i^2}$, the fluctuation of the temperature distribution becomes narrow, as has been pointed out.[7] One origin of the fluctuation could be the influence of sequential decay to the isotopes of interest. In order to correct such an effect, we introduce a correction factor, $k(A,Z)$, for each isotope yield by the relationship $Y_0(A,Z) = Y(A,Z)/k(A,Z)$, where $Y_0(A,Z)$ is the original isotope yield before the sequential decay. If we know exact values of $k(A,Z)$ and calculate the temperatures using corrected yields Y_0, the fluctuation should be significantly reduced.

We took a phenomenological approach to evaluate $k(A,Z)$, which could narrow the temperature distribution. Since the fluctuation arising from the sequential decay should

also appear for other reactions, we studied not only our inclusive results at 34°, but also inclusive data from FNAL($80 - 350 GeV/c\ p + Xe$ at 34°)[8] and MSU ($35 MeV/nucleon\ N + Ag$ at 38°)[9] experiments. In the MSU experiment, an emission temperature of 4.0±0.5 MeV was extracted from the relative populations of the excited states. By adjusting seven $k(A,Z)$ factors, which were set to be common for all reactions, we attempted to minimize any variance around the most probable temperature T_0 for each reaction. The temperatures were calculated from all combinations with $\delta B > 5$ MeV. Since the emission temperature was known for the MSU experiment, we set that the T_0 for the MSU experiment must be around 4.0 ± 0.4 MeV. The resultant $k(A,Z)$ factors are summarized in Table 1. T_0 and the standard deviation of the temperature distribution (RMS) for each reaction obtained for δB >5 MeV are also listed in Table 2.

Strictly speaking, the correction factor $k(A,Z)$ would not be common for all reactions, because of the different freeze-out temperatures in different reactions. The $k(A,Z)$ strongly depends on the excited-state populations, which may be affected by the freeze-out temperature. Therefore, we must be cautious to apply these common $k(A,Z)$ values to significantly high-temperature reactions. It should be noted, however, that the remaining fluctuation after introducing a common $k(A,Z)$ could not be removed, even using individual $k(A,Z)$ for each reaction. Considering the fact that some reaction shows a very sharp temperature distribution after a correction, the large remaining fluctuation for the other reactions must be caused by some kind of systematic error. We will use the RMS as a systematic error on the absolute value of the temperature extracted from the experimental data.

The obtained T_0 at 34° tends to increase as the target mass decreases. We can naively understand this tendency by relating the total energy deposition per target mass to the energy density in the emission source. Since the total energy deposition would be proportional to the path length of the projectile-proton in the target nucleus, this value per target mass might be roughly inversely proportional to $A_{target}^{2/3}$. Therefore, the lighter is the target nucleus we expect an emission source with the higher energy density. T_0 also seems to decrease as the proton energy increases from 8 GeV to 12 GeV. This might be due to the

energy dependence of the nuclear stopping power,[10] but more theoretical studies are needed to achieve a quantitative understanding on both trends.

In order to obtain temperatures and nucleon densities as a function of the emission angle without any complication, we selected only one combination of three single ratios, namely $Y_0(^9Li)/Y_0(^7Li)$, $Y_0(^7Be)/Y_0(^7Li)$, and $Y_0(^{10}Be)/Y_0(^9Li)$. This combination has the largest δB of 12.1 MeV and provides a temperature similar to T_0 at 34°. The multi-ratio R_{multi} in Eq. (3) can be written as

$$R_{multi} = \frac{Y_0(^9Li)^3 Y_0(^7Be)^2}{Y_0(^7Li)^3 Y_0(^{10}Be)^2}. \tag{6}$$

Typical angular distributions of the obtained temperatures are given in Fig. 3(a) for the $p+Au$ reaction at 8 GeV. The typical statistical errors are also indicated in the figure. Since we use Eq. (1) as the fragment yields, the angular distributions of the temperature can be obtained as continuous functions of the emission angle. As can be seen in the figure, the angular distributions have an anisotropic "U-Shape" for the temperature. There appears to be a small IMF-multiplicity dependence, implying either that there is a small correlation between the IMF-multiplicity and the impact parameter, or that the observed phenomena have a small impact-parameter dependence. The angular distributions of temperatures for the other two reactions at 8 GeV also show a similar tendency. It should be noted, however, that at 12 GeV their angular distributions are more like a "J-Shape", with higher temperatures at large emission angles and showing a non-negligible IMF-multiplicity dependence.

The absolute value of the obtained temperature was strongly restricted because we adopted common $k(A,Z)$ factors for all reactions, which could give a temperature for the MSU data within the constraint $T_0 = 4.0 \pm 0.4$ MeV. We may not refer to the obtained $k(A,Z)$ as the factor only for correcting the sequential decay effects, but also some other unphysical effects. Even though there may not be a real physical foundation, a correction with the above-mentioned procedure is indispensable to sharpen the temperature distributions.

Using Eqs. (4) and (5), we can also estimate the free-nucleon density. The total free-

nucleon density, defined as $\rho_{tF} = \rho_{pF} + \rho_{nF}$, is plotted in Fig. 3(b) for the $p+Au$ reaction at 8 GeV. Again, we find a "U-Shape" angular distribution for the free-nucleon density. These results are quite natural, assuming thermal and chemical equilibration of a mixed ideal gas of the fragment and nucleon. In such a case, more nucleons should exist as free nucleons in a higher temperature environment. This fact implies that the fragment density should be relatively large at a small free-nucleon density region. To take a simple analogical example, more liquid water may be formed at low temperature in a thermally equilibrated water and vapor system than at high temperature. The small free-nucleon density and the low temperature directly mean a high fragment (composite particle) density. Details concerning the analysis will be discussed elsewhere.[11]

The absolute value of the free-nucleon density is very small compared with the results of some theoretical calculation[12] and the experimental results measured by the particle-correlation method,[13] while similarly small values were obtained with the Quantum Statistical Model.[14] Recently, Albergo and Tricomi pointed out that a small value of the density may arise from the ideal-gas approximation, neglecting any residual nuclear interactions.[6] The nuclear binding energies used in Eqs. (4) and (5) should be modified in order to take into account the effects of surrounding hot nuclear medium. Albergo and Tricomi remedied the defect of the approximation by replacing $B(A,Z)$ in (2) with $B'(A,Z) = B(A,Z) - B_s A^{2/3}$, where B_s is a nuclear surface energy parameter which depends only on the density of the emission source.[6] Following the same prescription, we could obtain a slightly large value for the free nucleon density, as shown in Fig. 3(b). The improvement factor, $\rho_{tF}(B_s)/\rho_{tF}(B_s = 0)$, shows a strong temperature dependence. It could be as large as the order of magnitude for a small T (2-3 MeV), but is quite small for $T > 4$ MeV. Since an extracted temperature of around 4 MeV for the present work is strongly constrained by the results of the particle-correlation experiment at MSU, we cannot expect much improvement on the small-density estimation.

The ratios between the free-proton and -neutron density, $r = \rho_{pF}/\rho_{nF}$, turned out to be about 0.15 with a small angular dependence. The free-proton density could be smaller than

that for neutron, but the ratio r should be much closer to one. Obviously, further theoretical investigations concerning the free-nucleon densities are desired.

The anisotropic angular distributions of the temperature and density clearly indicate that a chemical freeze out is established before the entire remnant reaches thermal equilibrium. What must be noticed is that a high temperature appears not only at backward angles, but even at forward angles. We propose the following view as a possible explanation for these findings. The projectile proton drills a hole through the target nucleus and knocks out some nucleons along its passage. Finally, the remnant may appear toroid-shaped or partial eclipse-shaped, depending on the impact parameter.[15] Since a hot zone along the hole is surrounded by a cold nuclear medium at the beginning, U-Shape angular distributions of the temperature and of the free-nucleon density, and a nonuniform "stable" fragment density in the emission source would appear as a natural consequence. Though a sideward-enhanced fragment density has been introduced into the calculation for light stable isotopes from the beginning, because of the assumption $\rho(A,Z) \propto Y(A,Z)$, the shape difference of the angular distribution among the isotope yields plays an essential role to create an anisotropic angular distribution of the temperature and density. The resultant U-Shape angular distribution clearly proves that there should not be uniform temperature and density distributions in the fragment emission source. Since the nature of the observed angular distributions for the IMFs is mainly determined by that for stable isotopes, the nonuniform fragment density distribution must be the origin of the sideward-yield enhancement of the fragments.

Using the isotope-yield ratio, we cannot directly measure the maximum temperature produced during the early stage of a nuclear collision when the system is assumed to be in the complete gas phase. The reported caloric curve[2] suggests, however, that the temperature at the freeze-out timing could still have information at the hottest timing of the collision. The facts that some of the observed temperatures show non-constant values over 5 MeV, and that they have some target-mass dependence, could be an indication of the existence of a hot gas phase in the collision, since there should be a linear relationship between the temperature and the excitation energy at the gas phase. There is very attractive room for

further theoretical studies both on the fragmentation dynamics and the collision dynamics.

In summary, we have studied the isotope-yield ratios resulting from 8-GeV and 12-GeV proton-induced target multi-fragmentation reactions. The freeze-out temperature and free-nucleon density as a function of the fragment emission angle have been derived from the isotope-yield ratios. A new procedure has been described for suppressing the fluctuations in isotope temperatures. "U-Shape" angular distributions have been observed for both the temperature and the free-nucleon density, suggesting that there are nonuniform temperature and density distributions in the emission source of IMFs. These nonuniform distributions could be the origin of the sideward-peaked angular distributions for the heavier IMFs. More studies are, however, needed to draw any definite conclusion concerning the sideward peaking phenomena.

This work was supported in part by a Grant-in-Aid for Scientific Research (C) (No. 06640423 and No. 06640389) of the Japan Ministry of Education, Science, Sports and Culture (Monbusho). Some of authors (Murata, Mihara, Yasuda) acknowledged the receipt of the JSPS Research Fellowships for Young Scientists.

REFERENCES

1. W. Benenson, D.J. Morrisey, and W.A. Friedman, Ann. Rev. Nucl. and Part. Science, **44**, 27 (1994).
2. J. Pochodzalla et al., Phys. Rev. Lett. **75**, 1040 (1995).
3. S. Albergo et al., Nuovo Cimento A **89**, 1 (1985); A **101**, 815 (1989).
4. K. H. Tanaka et al., Nucl. Phys. A **583**, 581 (1995); T. Murakami et al., Perspectives in Heavy Ion Physics (World Scientific, Singapore, 1996), p. 152.
5. H. Ochiishi et al., Nucl. Instrum. Methods A **369**, 269 (1996).
6. S. Albergo and A. Tricomi, in Proc. of XXXVI Int. Winter Meeting on Nucl. Phys., Bormio, Italy, 1998 (edited by I. Iori); S. Albergo (private Communication).
7. M.B. Tsang et al., Phys. Rev. Lett. **78**, 3836 (1997).
8. A.S. Hirsh et al., Phys. Rev. C **29**, 508 (1984).
9. T. Nayak et al., Phys. Rev. C **45**, 132 (1992); T. Murakami (private communication).
10. J. Cugnon, Nucl. Phys. A **462**, 751 (1987).
11. J. Murata, PhD thesis, Kyoto University, 1999.
12. L.P. Csernai et al., Phys. Rev. C **28**, 2001 (1983).
13. H.A. Gustafsson et al., Phys. Rev. Lett. **53**, 544 (1984).
14. J. Pochodzalla et al., Phys. Rev. C **35**, 1695 (1987).
15. T. Maruyama and K. Niita, Prog. Theor. Phys. **97**, 579 (1997).

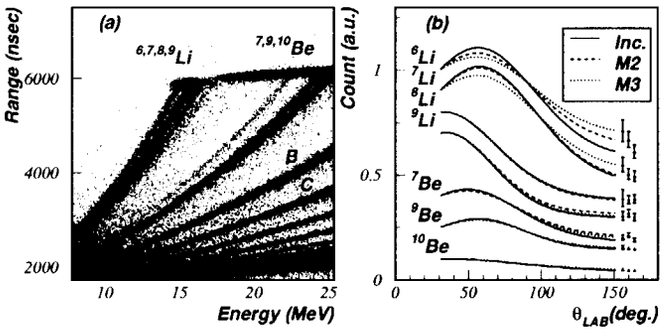

Fig. 1. Typical Range vs. Energy scatter plot (left) and angular distributions of the Li and Be isotopes for the $p + Au$ reaction at 8 GeV (right). Typical errors are also shown.

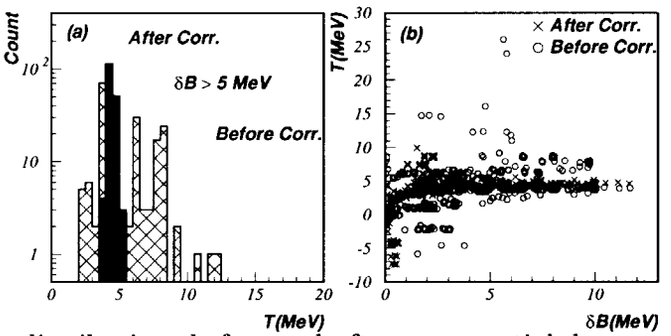

Fig. 2. Temperature distributions before and after a sequential decay correction for the 8 GeV $p + Au$ reaction. Temperature distribution of δB >5 MeV (left) and temperatures as functions of δB (right).

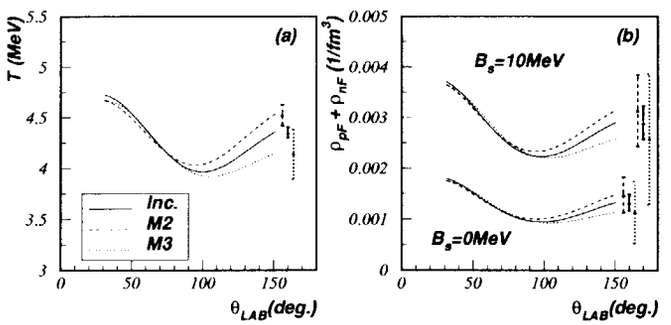

Fig. 3. Angular distributions of temperature (left) and free nucleon density (right) with ($B_s = 10$ MeV) and without ($B_s = 0$ MeV) the binding- energy variation effect for the $8GeV$ $p+Au$ reaction. Typical statistical errors are shown by error bars.

TABLES

Table 1. Yield correction factor for each isotope. $k(A,Z)$ was normalized as $k(^7Be) = 1$.

	^6Li	^7Li	^8Li	^9Li	^7Be	^9Be	^{10}Be
$k(A,Z)$	0.25	0.19	0.12	0.052	1	0.11	0.39

Table 2. The most probable temperatures $T_0(MeV)$ and standard deviations of temperature distributions $RMS(MeV)$.

	$8GeVp + A^a$			$12GeVp + A^b$				FNAL[c]	MSU[d]
	Au	Sm	Ag	Au	Tm	Sm	Ag		
T_0	4.1	5.9	5.8	3.6	4.3	5.3	5.0	4.8	3.6
RMS	0.30	0.44	0.20	0.21	0.66	0.29	0.36	0.34	0.26

[a,b]Present results estimated for $\theta_{LAB} = 34°$.

[c]FNAL result (80-350 GeV/c $p + Xe$, $\theta_{LAB} = 34°$).[8]

[d]MSU result (35 MeV/nucleon $N + Ag$, $\theta_{LAB} = 38°$).[9]

T_0 for MSU was forced to be around 4.0±0.4 MeV.